



HAL
open science

New insights into hydrogen permeation in steels : measurements through thick membranes

J. Kittel, F. Ropital, J. Pellier

► **To cite this version:**

J. Kittel, F. Ropital, J. Pellier. New insights into hydrogen permeation in steels: measurements through thick membranes. Corrosion 2008, Mar 2008, New-Orleans, United States. hal-02475533

HAL Id: hal-02475533

<https://ifp.hal.science/hal-02475533>

Submitted on 12 Feb 2020

HAL is a multi-disciplinary open access archive for the deposit and dissemination of scientific research documents, whether they are published or not. The documents may come from teaching and research institutions in France or abroad, or from public or private research centers.

L'archive ouverte pluridisciplinaire **HAL**, est destinée au dépôt et à la diffusion de documents scientifiques de niveau recherche, publiés ou non, émanant des établissements d'enseignement et de recherche français ou étrangers, des laboratoires publics ou privés.

NEW INSIGHTS INTO HYDROGEN PERMEATION IN STEELS: MEASUREMENTS THROUGH THICK MEMBRANES.

J. Kittel, F. Ropital, J. Pellier
IFP-Lyon
Rond-point de l'échangeur de Solaize - BP3
69390, Vernaison (FRANCE)

ABSTRACT

The permeation of hydrogen in steel in the presence of acid gases is not a simple phenomenon as the steel may contain trapping sites and also because the permeation may be governed by surface reactions associated with corrosion. Recently, hydrogen permeation experiments carried out at corrosion potential have shown a constant flux for various membrane thicknesses in the range 0.05 – 0.8 mm. This is in apparent contradiction with the Fick's laws of diffusion, predicting a diffusion flux inversely proportional to the thickness of the membrane. Such results confirm the possibility for permeation to be governed by surface reaction and not by the diffusion through steel: this situation corresponds to a *thin membrane* case. For thicker membranes it is expected that diffusion mechanisms through the steel is the rate determining step, so that the flux proportionality with the inverse of the membrane thickness is recovered. Nevertheless, it seems also that the limit between *thin membrane* and *thick membrane* situations is not universal, but depends strongly on the hydrogenating media: previous studies in sour service environments showed that 1 mm membranes could still be considered as thin, i.e. controlled by the interfacial fluxes rather than by the diffusion flux.

All these results reveal the difficulty to express the flux for thicker steel membrane (i.e. pipe) from laboratory studies on thin membranes, as the classical rule (flux proportional to the inverse of the membrane thickness) is not always applicable and not conservative.

This paper presents new permeation results, obtained on steel membranes up to 10mm thick. The transition between thin and thick membrane is clearly established, and is in the millimeter range in sour conditions. The necessity to adopt a new interpretative framework to link permeation measurements and hydrogen cracking mechanisms is reinforced. For thin membranes, the permeation flux is constant and governed only by the charging flux crossing the entry face. This surface mechanism is probably correlated with surface cracking mode, like SSC. On the other hand, the traditional concept of diffusion can only be used in thick membrane situations. The diffusion flux is inversely proportional to the sub-surface concentration. This concentration is in direct relation with the hydrogen activity in the steel, which is probably correlated with internal cracking modes, like HIC.

Keywords: Hydrogen permeation, H₂S, Hydrogen embrittlement, HIC, SSC

INTRODUCTION

Hydrogen damage is one of the major causes of steel equipment failures in the oil & gas industry. It is caused by the dissolution of hydrogen in the steel, as a result of the cathodic reduction of H^+ which accompanies the anodic oxidation of iron in acid media. The reduction of water molecules by cathodic overprotection is another potential source of reduced H^+ . Several failure modes can occur in service, for example:

- hydrogen induced cracking (HIC), corresponding to internal cracks generated by the recombination of hydrogen to gaseous molecules at certain appropriate traps in the steel, like MnS inclusions or pearlite bands. This failure mode is strictly internal, and does not require an external stress.
- Hydrogen stress cracking (HSC), also designed as sulfide stress cracking (SSC) when H_2S is present: this cracking mode is generated from the surface of the steel and requires an applied stress.

The presence of H_2S is known to have an aggravating influence.

In this respect, measurements of hydrogen permeation through steel membranes is an interesting technique, as it allows to determine some important parameters like the diffusion coefficient and the hydrogen concentration in the metal.

Another issue of hydrogen permeation through steels was recently discussed for pipe-in-pipe applications¹. Pipe-in-pipe structures might be used when thermal insulation is required to assure flow. In such systems, the production fluid is transported in the internal pipe. The thermal barrier is achieved by a vacuum or insulating material in the annular space between the internal and external pipe. Then, if hydrogen permeates through the steel and enters the annulus, the thermal efficiency might be lost.

Hydrogen Permeation and Hydrogen Cracking Susceptibility

Hydrogen permeation measurements have long been used as an experimental method for the assessment of hydrogen cracking mechanisms, and especially through the determination of the concentration of dissolved hydrogen. Many authors have used electrochemical permeation measurements for laboratory evaluation of steel susceptibility to all forms of hydrogen induced cracking, either HIC² or SSC³⁻⁹. Other studies even used hydrogen permeation as a unique experimental technique, for comparing different thermal treatments^{10,11} for martensitic low carbon steels. More academic studies also used different permeation techniques for a discussion of sour environments severity towards HIC or SSC¹².

More recently, on-site monitoring by an air stream measurement device¹³ has also been made available. This apparatus has been applied on-site for the evaluation of refinery equipment^{14,15}, pressure vessels¹⁶ or for wet sour gas pipelines¹⁷. It was also used for laboratory studies on thick steel membranes¹⁸⁻²⁰.

Most of the aforementioned studies were made with the assumption that the Fick's laws of diffusion can be applied. Considering one-dimensional diffusion, the ratio between the permeation transient $J(t)$ and the steady-state flux J_{ss} corresponding to the second Fick's law depends only on the diffusion coefficient D and the membrane thickness L :

$$\frac{J(t)}{J_{ss}} = 1 + 2 \sum_{n=1}^{\infty} (-1)^n \exp\left(-n^2 \pi^2 \frac{D \times t}{L^2}\right) \quad (1)$$

The diffusion coefficient may then be calculated from the transient curve using for example the time lag method (t_{lag} corresponds to the time at $J(t) / J_{ss} = 0.63$):

$$D = \frac{L^2}{6 \times t_{lag}} \quad (2)$$

Another method of calculation is based on the breakthrough time (t_b corresponds to the elapsed time measured extrapolating the linear portion of the rising transient to $J(t) = 0$):

$$D = \frac{L^2}{15.3 \times t_b} \quad (3)$$

With these assumptions, the hydrogen diffusion coefficient and the sub-surface concentration of hydrogen in the steel can be calculated, and some correlations with HIC and/or SSC can be examined.

However, recent results published by Crolet and co-workers pointed out the need to revisit the interpretation of permeation experiments^{12,21-23}. A new hydrogen charging mechanism and the corresponding modeling of permeation data were proposed.

In the light of the new mechanism, permeation measurements were modeled considering four hydrogen fluxes through a test membrane (*Figure 1*):

- at the entry face: the charging flux J_{ch} and a physical degassing flux J_{deg} ,
- Inside the material, the diffusion flux J_{diff} through the specimen,
- at the exit face, the extraction flux J_{ext} , which could either correspond to physical degassing (J_v) for permeation measurements in vacuum or air, or to an anodic extraction flux (J_a) for electrochemical measurements. Considering that the extraction method is "ideal", the hydrogen flux measured at the exit face is then equal to the diffusion flux.

Once the steady state has been reached, the mass balance at the entry face gives:

$$J_{ch} - J_{deg} = J_{diff} \quad (4)$$

Three cases can then be encountered:

- **in the absence of permeation through the steel** (practical case of a specimen totally immersed in the solution), the steady state diffusion flux through the steel (J_{diff}) is null. Thus, considering the entry face, the charging flux is completely balanced by the degassing flux. The concentration of dissolved hydrogen C_0 is constant and proportional to the square root of the charging flux.

$$J_{diff} = 0 \quad (5)$$

$$J_{ch} = J_{deg} \quad (6)$$

$$C_0 = \sqrt{J_{ch}/\alpha} \quad (7)$$

- **in a thick membrane situation**, the diffusion through the steel is the rate determining step, and permeation causes only a small disturbance at the entry face. Then, the hydrogen concentration beneath the entry face is not modified as compared to the previous situation, and still equals C_0 . The boundary condition for the first Fick's law of diffusion is a constant

concentration beneath the entry face. Thus, the diffusion flux is inversely proportional to the membrane thickness L.

$$J_{\text{ch}} \approx J_{\text{deg}} \gg J_{\text{diff}} \quad (8)$$

$$J_{\text{diff}} = D \times C_0 / L \quad (9)$$

- **in a thin membrane situation**, the diffusion flux might approach the value of the charging flux. Then the physical degassing at the entry face might become negligible. The rate determining step is then the hydrogen entry itself. The diffusion flux becomes constant and independent of the membrane thickness. The boundary condition for the first Fick's law of diffusion is a constant flux at the entry face and through the membrane. Thus, the hydrogen concentration C^* beneath the entry face is proportional to the membrane thickness L.

$$J_{\text{ch}} \approx J_{\text{diff}} \gg J_{\text{deg}} \quad (10)$$

$$C^* = J_{\text{diff}} \times L / D < C_0 \quad (11)$$

According to this model, the hydrogen sub-surface concentration and the diffusion flux follow two parallel but opposite evolutions with the test membrane thickness (*Figure 2*):

- below the critical thickness, in a thin membrane situation, the sub-surface concentration of hydrogen is proportional to the thickness, and the diffusion flux is constant,
- above the critical thickness, in a thick membrane situation, the sub-surface concentration is constant and the diffusion flux is inversely proportional with the thickness.

Unfortunately, the critical thickness (d_{crit}) where the transition between thin and thick membrane situation arise is not universal, but depends on the environment (pH, pH_2S , ...) and also on the steel properties. From the practical point of view, extrapolation of permeation results using the Fick's law of diffusion can only be performed in the thick membrane region. It is therefore important to have an idea of the critical thickness for a given steel and a given environment.

According to this new theory, a clear distinction should then be made between:

- internal hydrogen effects, such as HIC, which are controlled by the activity of hydrogen in the steel, and should be evaluated through thick membrane permeation experiments,
- external hydrogen effects, such as SSC, which are controlled by the raw charging flux J_{ch} crossing the entry face, and should be evaluated with the aid of permeation measurements through thin membranes.

The interpretation of permeation data for most of the electrochemical laboratory studies to date also need to be taken with great caution: indeed, calculation of hydrogen concentration are often based on permeation measurements through 0.5 to 2.0 mm membranes, which might often behave like a thin membrane in sour conditions^{1,12,22,23}. Such calculations are then obviously erroneous, since the boundary condition for the Fick's calculations is no more a constant concentration, but a constant flux. Then the subsurface concentration is proportional to the membrane thickness. At least, the thick membrane behavior should be verified by checking that the permeation current is inversely proportional with the membrane thickness, and for two different thicknesses. Only under this condition is it possible to use the first Fick's law for the evaluation of the sub-surface hydrogen concentration. Unfortunately, the verification of this property is only rarely found in published papers¹⁹.

EXPERIMENTAL

Tested Materials

Two different API X65 steels were selected for the experimental program. The first one consisted in a sweet service LSAW pipe, 42 inches diameter and 1 inch (25.4 mm) thick. The second one consisted in a sour service hot rolled plate, 20 mm thick. Their microstructures are compared in *Figure 3* and *Figure 4* respectively. Their chemical composition is given in *Table 1*. Permeation membranes 70 x 70 mm² were machined from the raw materials, with thickness varying between 0.5 and 10 mm.

Corrosive medium

All solutions were prepared according to EFC16 document, solution A, and thus contained 5% sodium chloride and 0.4% sodium acetate.

The bubbling gas is either pure H₂S, or a mixture of CO₂ with 0.3 % to 10 % H₂S, in order to obtain H₂S partial pressure of 3 to 1000 mbar.

After a thorough deoxygenating step, the solution was saturated by bubbling gas at ambient pressure. The pH was then adjusted to desired level, and through addition of deaerated 1N hydrochloric acid or deaerated 1N sodium hydroxide NaOH. The solution was then poured into the charging chamber. When the permeation current was stable, or after a period of 24 hours, the pH was decreased. Most of the time, the experimental sequence consisted of three pH steps: 5.5 – 4.5 – 3.5. For some specific tests, the experimental cell was placed in an autoclave, in order to examine the impact of temperature. Some experiments at pH 3.5 were then done at 25, 40 and 55 °C.

Permeation measurements: electrochemical / air stream

Most of the permeation experiments were conducted with a Devanathan-Stachurski²⁴ cell (*Figure 5*) that was designed specially for thick specimens. The exposed surface area was 19.6 cm². The thickness of the specimen varied between 0.5 and 10 mm.

The experimental set-up consisted of two identical electrolytic cells separated by the steel membrane. The charging surface was left at the corrosion potential. The exit surface was coated with Pd²⁵⁻²⁷ and held in a 0.1 M NaOH solution at a potential of +600 mV *versus* the open current potential. Thus all the hydrogen atoms diffusing through the membrane were oxidized, this oxidation current providing a measure of the hydrogen permeation flux.

Some experiments were made using the air stream measurement technique, with a device (Hydrosteel⁽¹⁾ 7000) developed for industrial site monitoring^{13,17}. The charging cell was identical to the one used for the electrochemical permeation, but the detection cell was replaced by a collector plate connected to the measurement apparatus. Under this configuration, the exit surface was simply rinsed with ethanol and dried. No palladium coating was used.

Corrosion measurements: charging side

For some tests, the corrosion rate of the steel in the charging solution was evaluated through polarisation resistance (R_p) measurements. The experimental parameters were as follow:

- measurement of the open current potential (E_{oc} vs. saturated calomel electrode) for 30 seconds,
- potentiodynamic sweep from -25 mV/E_{oc} to +25 mV/E_{oc} at 1 mV/s

⁽¹⁾ Hydrosteel is a trade name from Ion Science Ltd, UK

- R_p measurement by linear regression between -10 mV/ E_{oc} to +10 mV/ E_{oc}

The corrosion current was then calculated with standard Tafel coefficients (120 mV/decade) using the Stern and Geary equation:

$$J_{corr} = \frac{1}{2.3} \times \frac{b_a \cdot b_c}{b_a + b_c} \times \frac{1}{R_p} \quad (12)$$

RESULTS

Verification of the results: comparison of electrochemical and air stream techniques

According to Crolet and Bonis comparing different permeation techniques¹², air stream measurements provide a greater stability than electrochemical permeation. It was shown that the extraction efficiency of their palladium coating was drastically decreased after one day of experiment.

In order to check the stability of our palladium coating, one experiment was made comparing electrochemical permeation and air stream measurements during the same test. For this specific test, two identical membranes (0.5 mm thick) of steel B (sweet service grade) were exposed to the test solution in the charging cell. The first steel membrane was connected to the electrochemical half-cell used for electrochemical measurements, as described above. This steel membrane was coated with palladium. The second steel membrane was connected to the air stream collector plate. This configuration allowed the comparison of electrochemical permeation and air stream measurement for two identical steel specimens submitted to the same charging solution.

For the sake of comparison, the proportionality between the flux units is given by:

$$J_{\text{electroch}} (\mu\text{A}\cdot\text{cm}^{-2}) = 112 \times J_{\text{airstream}} (\text{pL}\cdot\text{cm}^{-2}\cdot\text{s}^{-1}) \quad (13)$$

The permeation transient measured with both methods during this experiment is presented in *Figure 6*. The same order of magnitude of the flux can be estimated with both measurement techniques. Specifically, the steady state value measured by the electrochemical method under pH 3.5 is approximately $40 \mu\text{A}\cdot\text{cm}^{-2}$, equivalent to $4500 \text{pL}\cdot\text{cm}^{-2}\cdot\text{s}^{-1}$, which was obtained from the airstream technique. However, at lower pH, it appears that the efficiency of the airstream technique, as represented by the maximum flux, is lower than that of electrochemical extraction. On the other hand, the efficiency of the extraction technique decreases with time, resulting in pronounced flux maxima, not so evident from airstream flux profiles. These differences between air stream and electrochemical extraction could be an indication that this peak value is related to the exit face, which is not identical for both methods. More comparative experiments should be necessary to examine this in more details.

A second experiment was then repeated in exactly the same conditions, in order to verify the repeatability of the testing procedure. Unfortunately, the palladium coating on the membrane for electrochemical measurement had been omitted for this duplicate test. The permeation transient measured during this second experiment is given in *Figure 7*. The permeation flux as measured by the air stream method between both experiments is found to be repeatable (*Figure 6* and *Figure 7*). The steady-state current are respectively 120 and 180 $\text{pL}\cdot\text{cm}^{-2}\cdot\text{s}^{-1}$ at pH 5.5, 2100 and 2700 $\text{pL}\cdot\text{cm}^{-2}\cdot\text{s}^{-1}$ at pH 4.5, and 3400 and 3600 $\text{pL}\cdot\text{cm}^{-2}\cdot\text{s}^{-1}$ at pH 3.5. On the other hand, the electrochemical measurement with and without the Pd coating is not consistent. Extremely low permeation fluxes are measured without the coating, as compared with the Pd coated specimen tested under the same conditions.

The conclusions to these preliminary tests are the following:

- for a long term stability of the electrochemical measurements (several days), the application of a Pd coating on the exit face of the specimen is required,
- permeation fluxes measured by electrochemical means and air stream measurements are in good qualitative and quantitative agreement,
- the repeatability of permeation transients as measured by the air stream technique is correct.

For the remaining part of this study, all the experiments were performed with the electrochemical method.

Impact of p_{H₂S} and pH

The impact of H₂S partial pressure is illustrated in *Figure 8*, for permeation experiments on 1 mm thick membranes, tested at pH 5.5 with 0.3, 1 and 10 % H₂S balanced with CO₂ to a total pressure of 1 bar.

The impact of pH is illustrated in *Figure 9* for a test on 10 mm membrane (steel B) under 100 mbar H₂S / 900 mbar CO₂, with successive pH steps from 5.5 to 2.8.

As expected, the steady-state permeation flux increases with H₂S partial pressure and with pH. In order to quantify the impact of both parameters, all the diffusion fluxes measured during this study were plotted in log scales as a function of H₂S partial pressure (*Figure 10*) or as a function of pH (*Figure 11*).

The same analysis was performed for the corrosion rate. For each experimental condition (pH – p_{H₂S}), linear polarisation measurements were made in the charging cell. The corresponding results are presented in *Figure 12* for the influence of H₂S partial pressure and in *Figure 13* for pH.

A unique expression could be derived to express the permeation flux evolution with proton concentration and H₂S partial pressure:

$$J_{\text{perm}} \propto [\text{H}^+]^{0.25} \times [\text{H}_2\text{S}]^{0.17} \quad (14)$$

A law approximately similar was found for the corrosion rate, except that the pre-exponential factor was higher for steel grade A (higher corrosion):

$$J_{\text{corr}} \propto [\text{H}^+]^{0.2-0.25} \times [\text{H}_2\text{S}]^{0.17} \quad (15)$$

Quite remarkably, the permeation flux expression seems to be independent of the steel grade and of the membrane thickness. The comparison of these results with the literature is quite interesting. Asahi *et al.*³ have studied low carbon high strength steels, and found that J_{perm} was proportional to $[\text{H}^+ \times \text{H}_2\text{S}]^{0.25}$. A similar trend was observed by Boellinghaus *et al.*^{10,11} for 13 % chromium martensitic stainless steels, with a steady state permeation flux proportional to $[\text{H}_2\text{S}]^{0.16-0.25}$. Those results were later confirmed by Duval *et al.*¹ for ARMCO iron membranes, with an expression very close to that obtained during the present study. They also performed the same analysis for corrosion rate, through linear polarization measurements:

$$J_{\text{perm}} \propto [\text{H}^+]^{0.25} \times [\text{H}_2\text{S}]^{0.15} \quad (16)$$

$$J_{\text{corr}} \propto [\text{H}^+]^{0.25} \times [\text{H}_2\text{S}]^{0.2} \quad (17)$$

These results, obtained on thin membranes (0.5 – 1 mm) are in excellent agreement with the results of the present study, although the dependence with H₂S partial pressure was not extensively examined. It is also extremely interesting to see that permeation on thick membranes still follows the same pH dependency than on thin membranes. More remarkable is the apparent absence of impact of the balance gas. Indeed, all the previous results^{1,3,10,11} were obtained with H₂S / N₂ gas mixtures, whereas H₂S / CO₂ mixtures were used in the present work. This should give rise to completely different surface films. In the latter case, HS⁻ adsorption is in competition with HCO₃⁻, and a surface coverage of sulfide proportional to HS⁻/HCO₃⁻, i.e. proportional to p_{H₂S}/p_{CO₂} is expected²¹. Then, the strict observance of the direct hydrogen charging model through HS⁻ adsorbate would predict a [p_{H₂S}]¹ law²¹. According to Crolet²³ commenting the results of Asahi *et Al.*³, this dependence on (H⁺ x p_{H₂S})^{1/4} should result from an error bar in a reaction order of 0, rather than a really significant reaction order of ¼. New experiments in H₂S / N₂ gas mix and comparisons with H₂S / CO₂ mix should help clarifying this point.

Impact of temperature

The impact of temperature on corrosion and permeation was evaluated through experiments at pH 3.5 and under 10 % H₂S. The experimental cell was placed in an autoclave, and the temperature was progressively increased from 25 to 55 °C. A typical permeation transient is presented in *Figure 14*.

It has to be noted that gas saturation was always performed under atmospheric pressure: therefore, the partial pressure of H₂S is not rigorously the same for all experiments, as the water partial pressure at 25 °C is approximately 30 mbar, whereas it reaches 150 mbar at 55 °C. Nevertheless, considering that the permeation flux for our experimental conditions can be well described with expression (15), the deviation associated with the H₂S partial pressure change between 25 °C and 55 °C would be less than 5 %.

In order to check if corrosion and permeation present thermal activation trends, the results are plotted in log scale, versus the opposite of temperature (*Figure 15* and *Figure 16*).

Within this range of temperature, the evolutions of J_{corr} and J_{perm} seem to follow an Arrhenius law:

$$J = J_0 e^{\frac{-E_a}{RT}} \quad (18)$$

The values of the corresponding activation energies are approximately 22 kJ.mol⁻¹ for the permeation flux and 30 kJ.mol⁻¹ for the corrosion rate.

Previous results are in good agreement with activation energies values found in the literature for hydrogen diffusion coefficient, between 17 kJ.mol⁻¹²⁸ and 21 kJ.mol⁻¹²⁹. However, in the present study, only the diffusion flux was evaluated, and the individual contributions of the diffusion coefficient and of the sub-surface concentration of hydrogen could not be separated.

For corrosion rates in sour environment, no comparative results were found in the literature. The comparison with corrosion in CO₂ corrosion gave activation energies around 50 kJ.mol⁻¹³⁰.

Impact of Steel Membrane Thickness

The impact of membrane thickness on permeation transient is illustrated in *Figure 17*, for permeation experiments on steel A membranes of various thickness, tested at pH 5.5 under 100 mbar H₂S and 900 mbar CO₂.

As expected, the thickness increase resulted in a decrease in the steady-state permeation flux decreased and an increase in the breakthrough time.

In order to verify the transition between thick and thin membrane behavior, the permeation flux was plotted versus the opposite of the membrane thickness, for tests under 100 mbar H₂S and 900 mbar CO₂, at different pH and for both steel A and steel B (*Figure 18*). These experimental results accurately reproduce the theoretical predictions of *Figure 2*^{12,22}. The expected transition at d_{crit} is effectively observed, and occurred between 2 and 3 mm. Above this thickness, the permeation flux is inversely proportional to the membrane thickness. For thinner membrane, a constant flux is observed. These findings also confirm previous results of Duval *et al.*¹, who observed a *thin membrane* behavior up to 1.5 mm in comparable test solution. However, no clear demonstration of the transition between thick and thin membrane regimes was found in the literature to date.

A more detailed interpretation of these results can be made after calculation of the permeation efficiency:

$$E_p = J_{ch}/J_{diff} \quad (19)$$

This ratio was calculated as follows. For a given experimental condition, *i.e.* same material, same pH and same pH₂S, the charging flux is constant and is given directly by the flux measured in a thin membrane condition, provided that the extraction method is ideal. Then, for each material and test solution (pH, pH₂S), the permeation efficiency was calculated for each thickness as the ratio between the diffusion flux divided by the diffusion flux measured for a 0.5 mm membrane. The corresponding results are presented in *Figure 19*, for tests on steel A and steel B, with pH from 2.8 to 5.5, and under 100 mbar H₂S and 900 mbar CO₂.

From this result, it is quite clear that for a given gas composition, the permeation efficiency is homothetic, whatever the pH of the test solution between 2.8 and 5.5. The steel type does neither seem to have an impact, but both had the same microstructure (ferrite - pearlite), steel A being sour service and steel B sweet service. This means that for a given H₂S/CO₂, any pH change will have the same quantitative impact on the charging flux J_{ch} (equal to the diffusion flux measured on thin membrane) and on the hydrogen subsurface concentration C_0 (proportional to the diffusion flux measured on thick membrane). It would be extremely interesting to perform the same analysis for solutions with different H₂S concentration. Then, it will be possible to compare the respective impact of pH and pH₂S on SSC (presumably related to J_{diff}) and HIC (presumably related to C_0).

CONCLUSION

The measurements performed during this study represent the first experimental evidence of the thin to thick membrane behavior for hydrogen diffusion in sour conditions. As already forecasted^{1,22}, the critical thickness corresponding to this transition is in the millimeter range, and does not seem to depend much on the test solution pH from 2.8 to 5.5. The impact of H₂S was not quantified.

This result is of great value, as it confirms the model proposed by Crolet²² for the interpretation of permeation data. Below the critical thickness, the diffusion flux that is measured corresponds to the

charging flux, hence it may be expected to quantitatively relate to the severity of scenarios to cause SSC. Above the critical thickness, the diffusion flux is inversely proportional to the thickness and is therefore directly related to the sub-surface hydrogen concentration C_0 and hydrogen activity. This is one important parameter for the susceptibility of steel to HIC, though others are also thought to play a major role, such as the presence of particular species like MnS.

This confirms also that most of the past studies using hydrogen permeation for C_0 calculations were misinterpreted. Indeed, the vast majority used thin membranes, for which the measured flux is constant and equal to the charging flux. It can therefore not be used for the determination of C_0 , the result rather being an apparent sub-surface concentration C^* proportional to the thickness and to the measured flux. Thus, the correlation with SSC that was sometimes found was a correct result, but the interpretation was wrong: the result of a thin membrane permeation measurement is proportional to the charging flux, and not to the sub-surface concentration. But SSC is related to the charging mechanism, and not to internal hydrogen concentration.

As a complement to the results obtained during this study, the determination of the permeation efficiency for various membrane thickness and for other H_2S partial pressure would be of great interest: it would then be possible to study the pH – pH_2S severity domains, for both HIC and SSC: the former in the light of permeation results on thick membranes, giving access to C_0 , the latter in the light of permeation results on thin membranes, giving access to the charging flux.

ACKNOWLEDGMENTS

The authors would like to thank Frank Dean, of Ion Science Ltd, for his kind assistance with the use of the Hydrosteel 7000 device.

The contribution of Gilbert Parrain for the measurements in H_2S environments, and the comparisons between electrochemical and air stream permeation is also greatly acknowledged.

Table 1: chemical composition of tested steels (wt. %).

	C	Mn	Si	P	S	Cr	Ni	Mo	Cu	Al	Ti	Nb
steel A	0,046	1,36	0,322	0,008	0,001	0,041	0,036	0,008	0,047	0,036	0,019	0,045
steel B	0,09	1,56	0,28	0,014	0,001	0,05	0,03	0,01	0,02	0,030	0,000	0,040

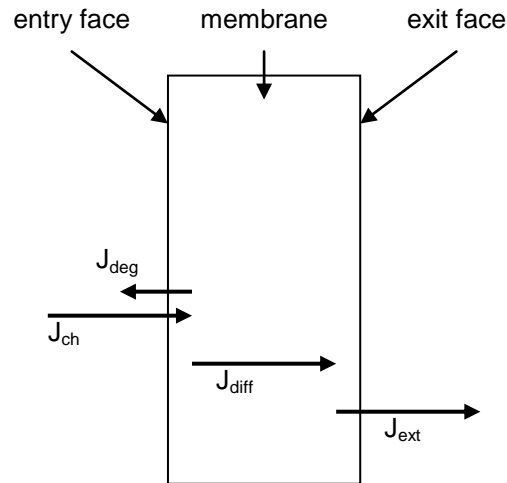


Figure 1: Different hydrogen fluxes through a steel membrane.

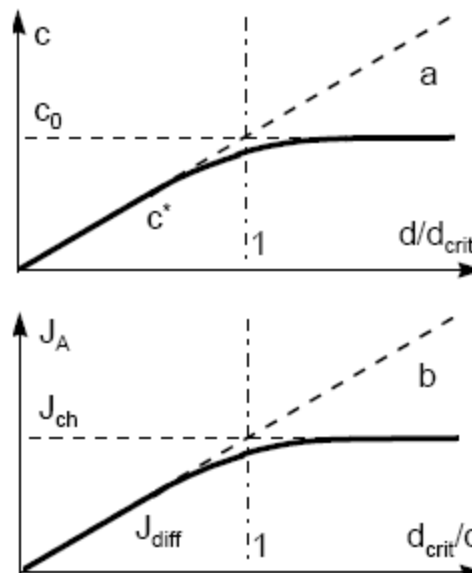


Figure 2: variation of (a) the hydrogen sub-surface concentration C , and (b) the permeation flux through the membrane J_A as a function of the normalized membrane thickness d / d_{crit} (from ref. 22).

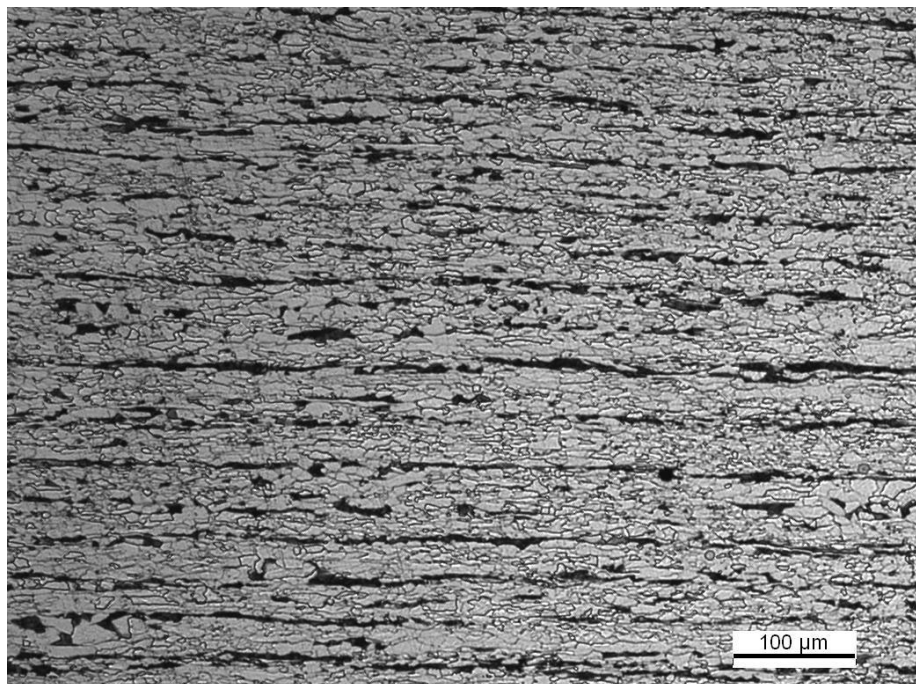


Figure 3: microstructure of the sweet service grade in the L direction.

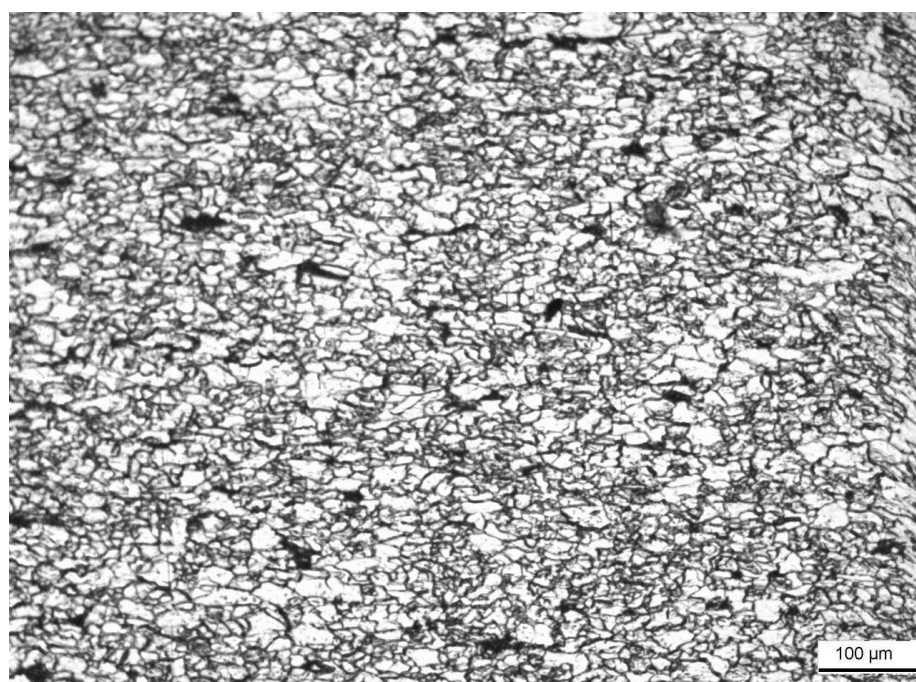


Figure 4: microstructure of the sour service grade in the L direction.

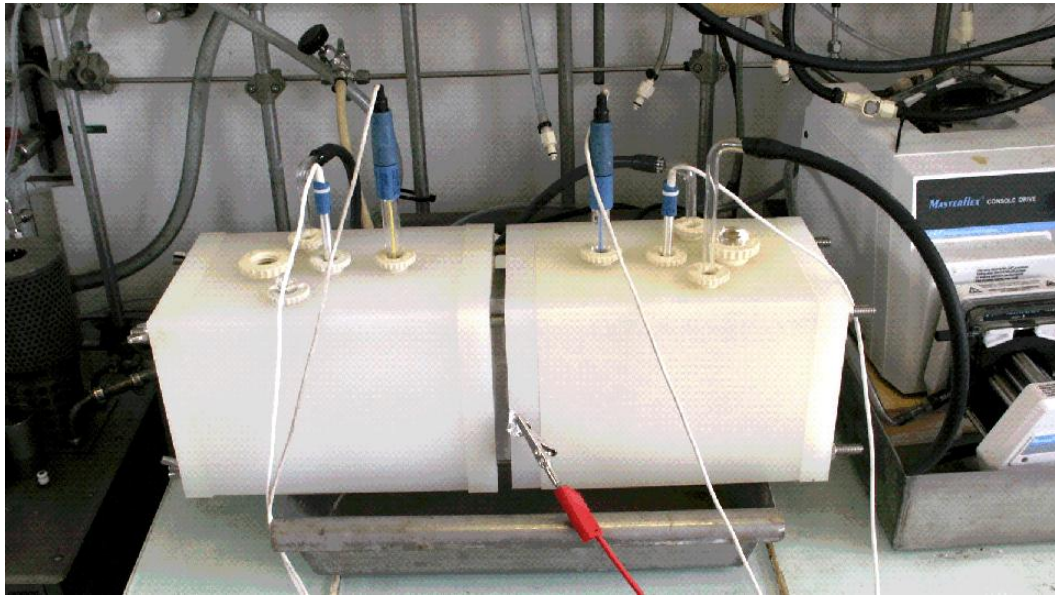


Figure 5: Devanathan-Stachurski cell for permeation measurements on thick specimens.

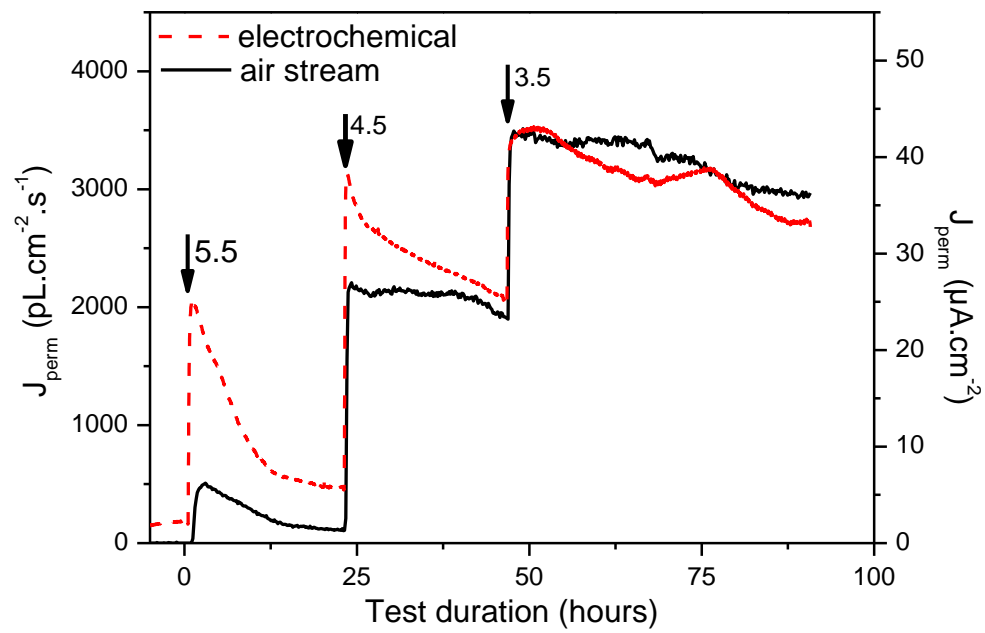


Figure 6: permeation transients measured simultaneously by air stream technique and electrochemical method, for two identical membranes (0.5 mm) of steel B exposed to test solution saturated with 1 bar H₂S, and with successive pH steps. Electrochemical membrane with Pd coating on the exit face.

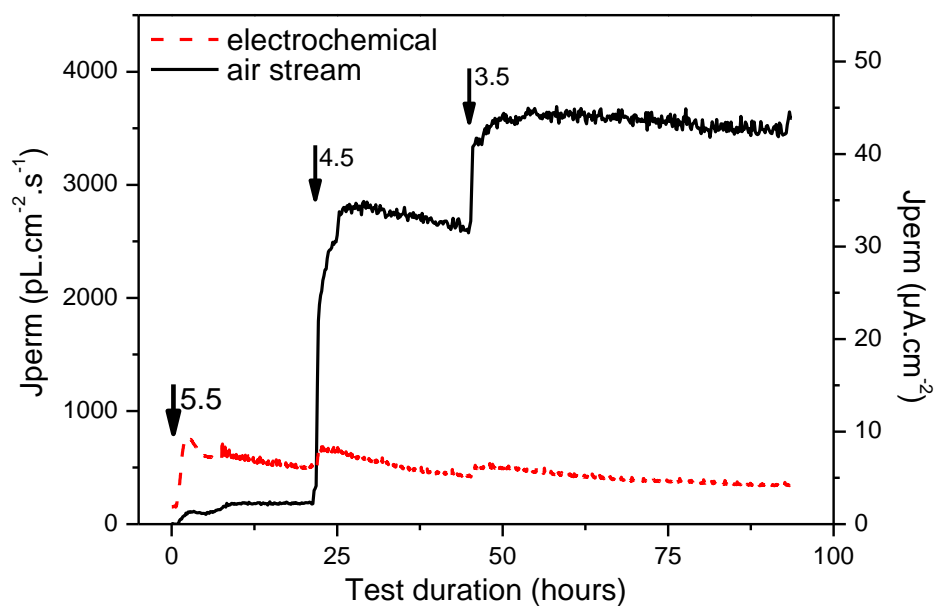


Figure 7: permeation transients measured simultaneously by air stream technique and electrochemical method, for two identical membranes (0.5 mm) of steel B exposed to test solution saturated with 1 bar H_2S , and with successive pH steps. Electrochemical membrane without Pd coating on the exit face.

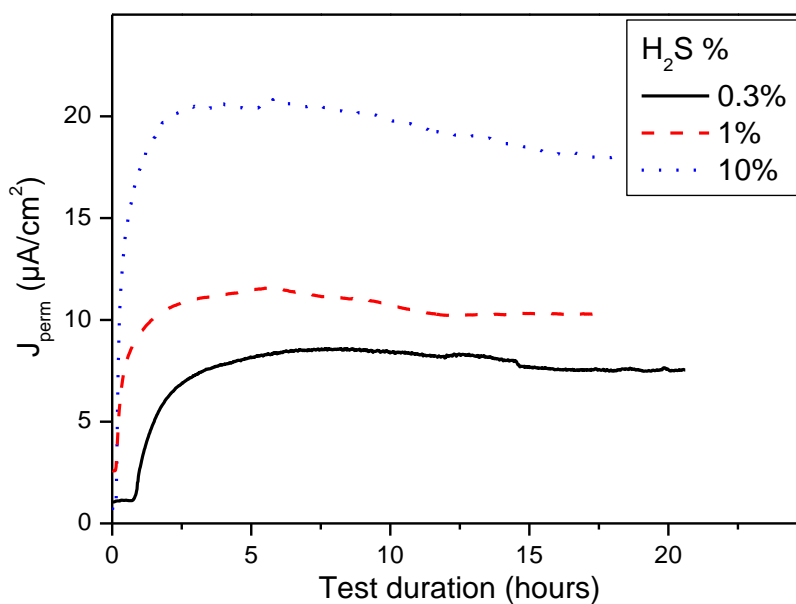


Figure 8: Permeation transients measured for 1 mm membranes of steel A exposed to test solution at pH 3.5 saturated under 1 bar with different H_2S / CO_2 ratios.

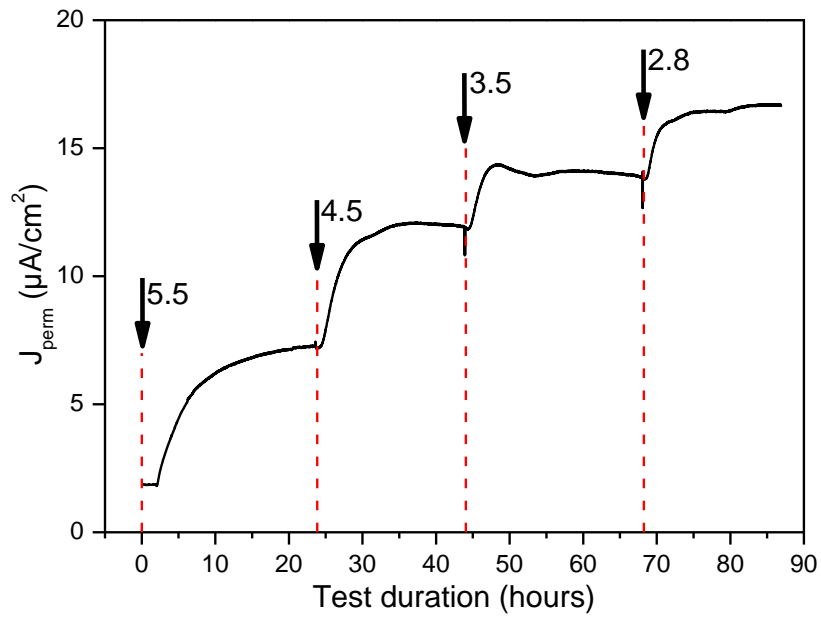


Figure 9: Permeation transient measured for a 10 mm membrane of steel B exposed to test solution at various pH 3.5 saturated under 100 mbar H_2S and 900 mbar CO_2 .

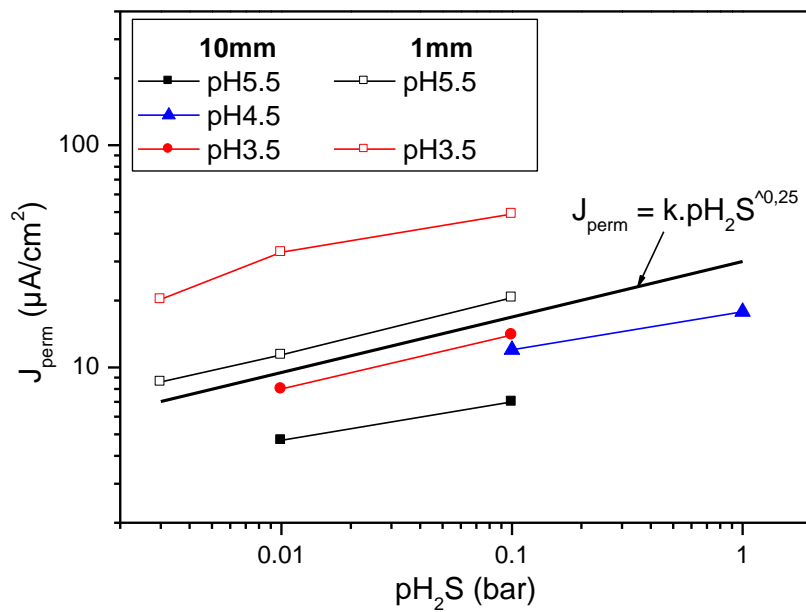


Figure 10: Evolution of the permeation flux with H_2S partial pressure (CO_2 balance to 1 bar) for different pH and membrane thicknesses (steel B).

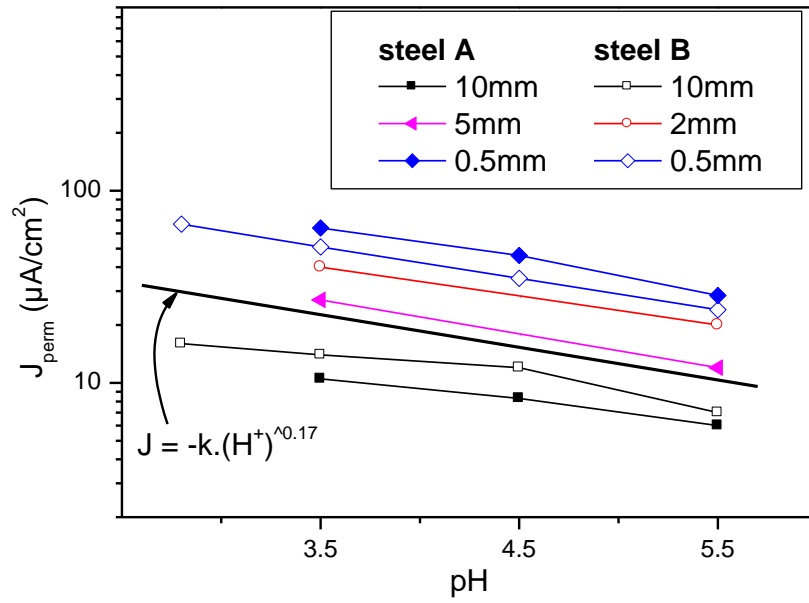


Figure 11: Evolution of the permeation flux with pH for experiments under 100 mbar H_2S and 900 mbar CO_2 , for different steel grades and different membrane thicknesses.

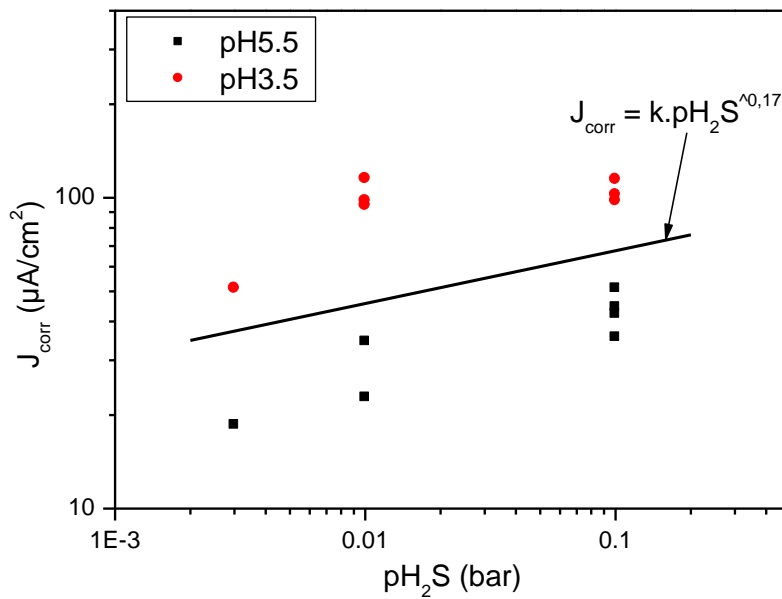


Figure 12: Evolution of the corrosion current density evaluated from R_p measurements as a function of H_2S partial pressure (CO_2 balance to 1 bar) and for different test solution pH (steel B).

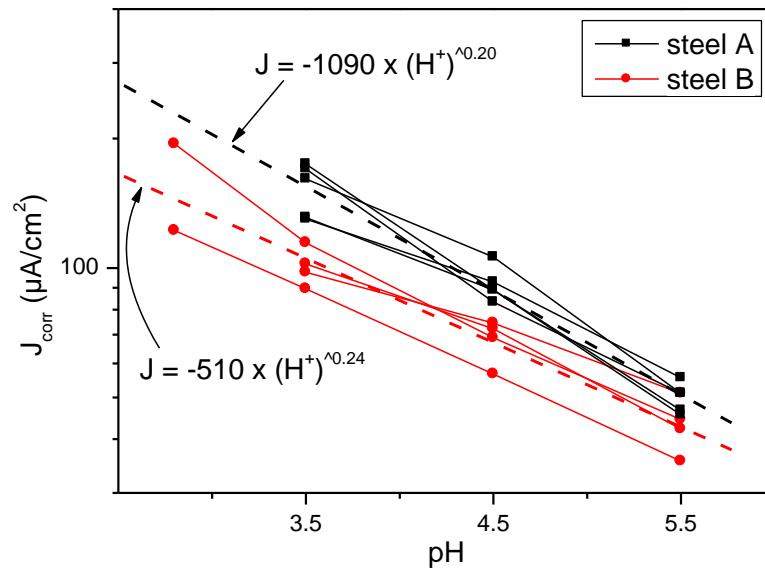


Figure 13: Evolution of the corrosion current density evaluated from Rp measurements as a function of pH and for experiments under 100 mbar H₂S and 900 mbar CO₂, for different steel grades.

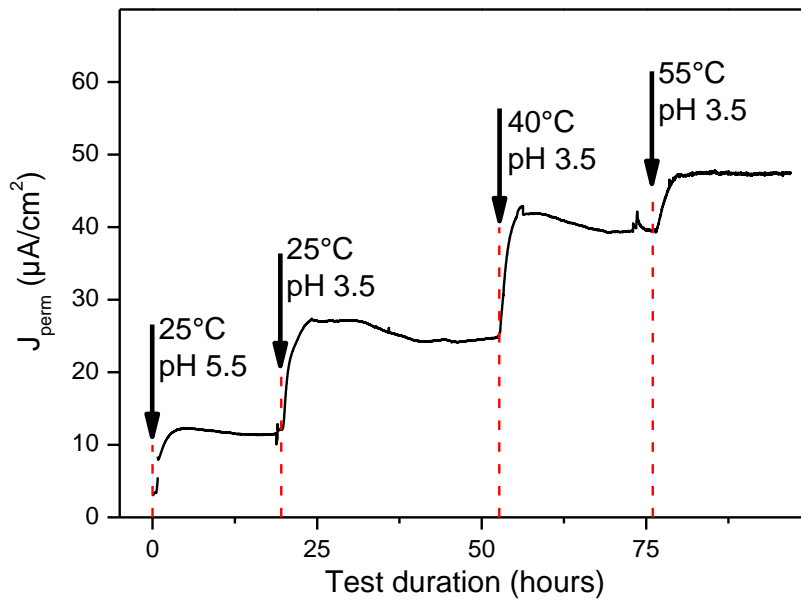


Figure 14: Impact of temperature on permeation transient measured for a 5 mm membrane of steel A exposed to test solution at various pH and under 100 mbar H₂S and 900 mbar CO₂.

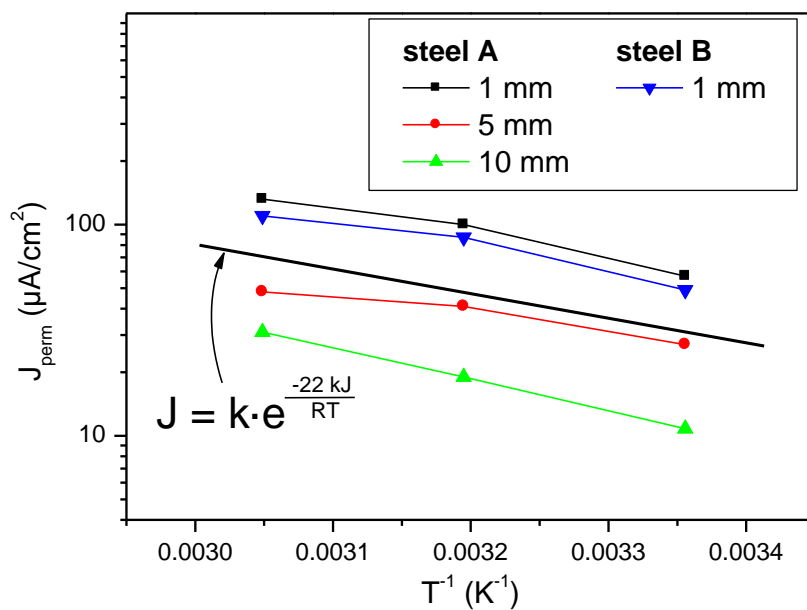


Figure 15: Evolution of the permeation flux with temperature, for different experiments at pH 3.5 under 10 % H_2S and 90 % CO_2 .

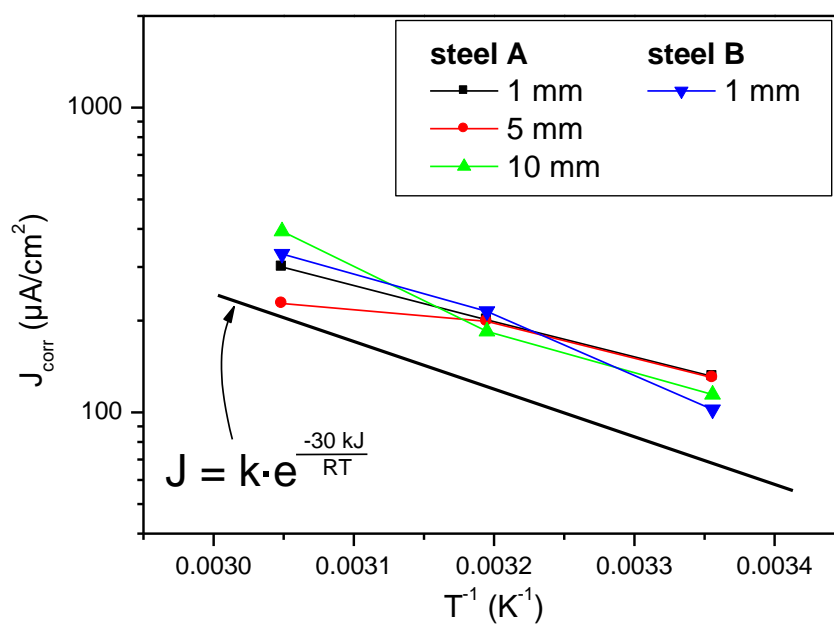


Figure 16: Evolution of the corrosion current with temperature, for different experiments at pH 3.5 under 10 % H_2S and 90 % CO_2 .

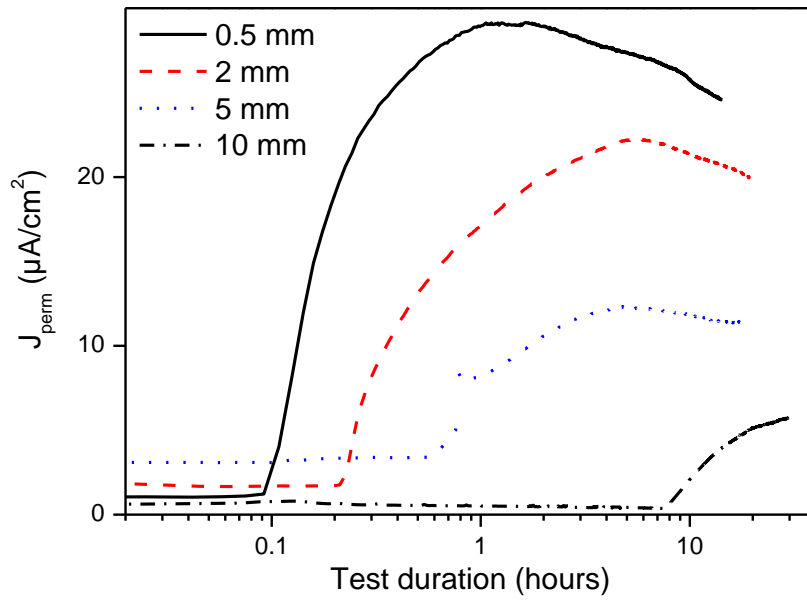


Figure 17: Permeation transients measured for steel A membranes of different thickness, exposed to test solution at pH 5.5 saturated with 100 mbar H_2S and 900 mbar CO_2 .

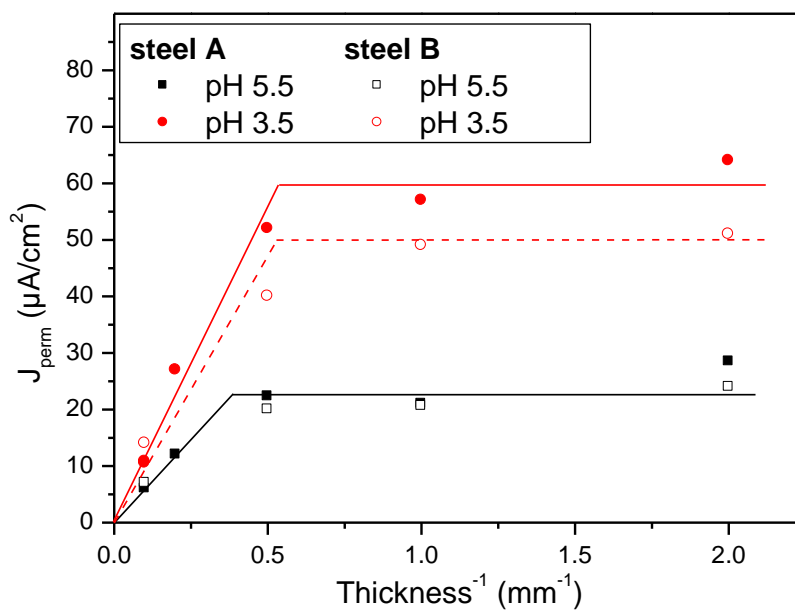


Figure 18: Evolution of permeation flux with membrane thickness for different experiments under 100 mbar H_2S and 900 mbar CO_2 .

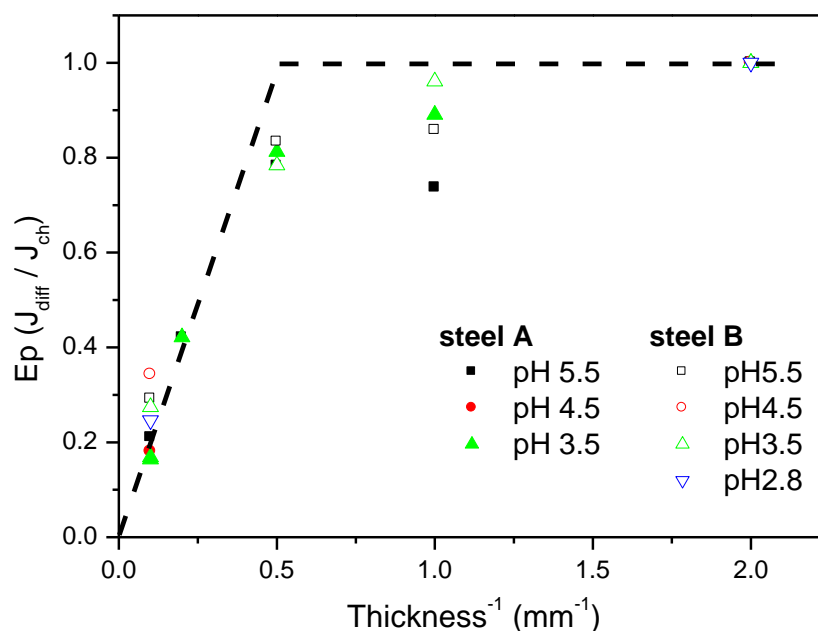


Figure 19: Evolution of permeation efficiency ($E_p = J_{diff} / J_{ch}$) with membrane thickness, for all experiments under 100 mbar H_2S and 900 mbar CO_2 .

REFERENCES

1. S.Duval, R.Antano-Lopez, C.Scomparin, M.Jerome, , F.Ropital,, "Hydrogen permeation through ARMCO iron membranes in sour media", Corrosion 2004, NACE Conf. Series, paper n°04740 (2004).
2. M.Kimura, N.Totsuka, T.Kurisu, T.Hane, Y.Nakai, "Effect of environmental factors on hydrogen permeation in line pipe steel", *Corrosion*, vol.44 n°10, 738-744 (1988)
3. H.Asahi, M.Ueno, T.Yonezawa, "Prediction of sulfide stress cracking in high-strength tubulars", *Corrosion* vol.50 n°7, 537-545 (1994)
4. S.U.Koh, J.S.Kim, B.Y.Yang, K.Y.Kim, "Effect of line pipe steel microstructure on susceptibility to sulfide stress cracking", *Corrosion* vol.60 n°3, 244-253 (2004)
5. S.U.Koh, B.Y.Yang, K.Y.Kim, "Effect of alloying elements on the susceptibility to sulfide stress cracking of line pipe steels", *Corrosion* vol.60 n°3, 262-274 (2004)
6. G.T.Park, S.U.Koh, K.Y.Kim, H.G.Jung, , "Effect of steel microstructure on hydrogen permeation behavior and the determination of critical hydrogen flux for hydrogen embrittlement", Corrosion 2006, NACE Conf. Series, paper n°06438 (2006)
7. J.Marsh, "Comparing hydrogen permeation rates, corrosion rates and sulphide stress cracking resistance for C-110 and P-110 casing steel", Corrosion 2007, NACE Conf. Series, paper n°07109 (2007)
8. C.Mendez, I.Martinez, L.Melian, J.Vera, "Application of hydrogen permeation for monitoring sulfide stress cracking susceptibility", Corrosion 2002, NACE Conf. Series, paper n°02342 (2002)
9. J.R.Vera, R.Case, A.Castro, "The relationship between hydrogen permeation and sulfide stress cracking susceptibility of OCTG materials at different temperatures and pH values", Corrosion 1997, NACE Confer. Series, paper n°97047 (1997)
10. T.Boellinghaus, H.Hoffmeister, K.Klemme, H.Alzer, "Hydrogen permeation in a low carbon martensitic stainless steel exposed to H_2S containing brines at free corrosion", Corrosion 1999, NACE Conf. Series, paper n°99609 (1999)

11. T.Boellinghaus, H.Hoffmeister, "hydrogen permeation in supermartensitic stainless steels dependent on heat treatment and chemical composition", *Corrosion 2000*, NACE Conf. Series, paper n°00141 (2000)
12. M.R.Bonis, J-L.Crolet "Permeation measurements on thin steel membranes", *Corrosion 2002*, NACE Conf. Series, paper n°02036 (2002)
13. F.W.H.Dean, D.J.Fray, "Ultrasensitive technique for detection of hydrogen emanating from steel and other solid surfaces", *Materials Sci. and Technol.*, vol.16, 41-46 (2000)
14. A.D.Ethridge, E.B.McDonald, D.G.Serate, F.W.H.Dean, "Examples of use and interpretation of field data using a portable hydrogen permeation monitor", *Corrosion 2004*, NACE Conf. Series, paper n°04477 (2004)
15. F.W.H.Dean, S.W.Powell, "Hydrogen flux and high temperature acid corrosion", *Corrosion 2006*, NACE Conf. Series, paper n°06436 (2006)
16. F.W.H.Dean, M.J.Carroll, and P.A.Nutty, "Hydrogen permeation flux data correlation with in-line corrosion monitoring techniques mapped over location and time", *Corrosion 2001*, NACE Conf. Series, paper n°01636 (2001)
17. R.D.Tems, F.W.H.Dean, "Filed application of a new, portable, non-intrusive hydrogen monitor for sour service", *Corrosion 2000*, NACE Conf. Series, paper n°00471 (2000)
18. F.W.H.Dean, S.W.Powell, "A laboratory study of types of corrosion inducing hydrogen permeation through steel", *Corrosion 2004*, NACE Conf. Series, paper n°04472 (2004)
19. F.W.H.Dean, "Measurement of hydrogen permeation through structural steel sections of varying thickness at 19 degrees C", *Materials Science and Technology* vol.21 n°3, 347-351 (2005)
20. S.J.Mishael, F.W.H.Dean, C.M.Fowler, "Practical applications of hydrogen permeation monitoring", *Corrosion 2004*, NACE Conf. Series, paper n°04476 (2004)
21. J-L.Crolet, G.Maisonneuve, "Construction of a universal scale of severity for hydrogen cracking", *Corrosion 2000*, NACE Conf. Series, paper n°00127 (2000)
22. J-L.Crolet, M.R.Bonis, "Revisiting hydrogen in steel, part I: theoretical aspects of charging, stress cracking and permeation", *Corrosion 2001*, NACE Conf. Series, paper n°01067 (2001)
23. J-L.Crolet, M.R.Bonis, "Revisiting hydrogen in steel, part II: experimental verifications", *Corrosion 2001*, NACE Conf. Series, paper n°01072 (2001)
24. M.A.V.Devanathan, Z.Stachurski, "The mechanism of hydrogen evolution on iron in acid solutions by determination of permeation rates", *J. Electrochemical Soc.*, vol.111 n°5, 619-623 (1964)
25. P.Manolatos, M.Jerome, "A thin palladium coating on iron for hydrogen permeation studies", *Electrochimica Acta*, vol.41 n°3, 359-365 (1996)
26. P.Manolatos, M.Jerome, J.Galland, "Necessity of A Palladium Coating to Ensure Hydrogen Oxidation During Electrochemical Permeation Measurements on Iron", *Electrochimica Acta*, vol.40 n°7, 867-871 (1995)
27. P.Manolatos, M.Jerome, C.Duret-Thual, J.Le Coze, "The electrochemical permeation of hydrogen in steels without palladium coating. Part I: Interpretation difficulties", *Corrosion Science*, vol.37 n°11, 1773-1783 (1995)
28. F.W.H.Dean, T.M.Smeeton, D.J.Fray, "Hydrogen permeation through mild steel in temperature range 20-500 degrees C measured by hydrogen collection method", *Materials Sci. and Technol.*, vol.18 n°8, 851-855 (2002)
29. R.W.Revie, V.S.Sastri, M.Elboujdaini, R.R.Ramsingh, Y.Lafrenière, "Hydrogen-induced cracking of line pipe steels used in sour service", *Corrosion*, vol.49 n°7, 531-535 (1993)
30. "Predicting CO₂ corrosion in the oil and gas industry", EFC publication n°13, The Institute of Materials, London, UK (1994)